

# UCSF

## UC San Francisco Previously Published Works

### Title

The Brain Chart of Aging: Machine-learning analytics reveals links between brain aging, white matter disease, amyloid burden, and cognition in the iSTAGING consortium of 10,216 harmonized MR scans

### Permalink

<https://escholarship.org/uc/item/7jn344p2>

### Journal

Alzheimer's & Dementia, 17(1)

### ISSN

1552-5260

### Authors

Habes, Mohamad  
Pomponio, Raymond  
Shou, Haochang  
et al.

### Publication Date

2021

### DOI

10.1002/alz.12178

Peer reviewed



Published in final edited form as:

*Alzheimers Dement.* 2021 January ; 17(1): 89–102. doi:10.1002/alz.12178.

## The Brain Chart of Aging: Machine learning analytics reveals links between brain aging, white matter disease, amyloid burden and cognition in the iSTAGING consortium of 10,216 harmonized MR scans

Mohamad Habes, PhD<sup>1,2,21,\*</sup>, Raymond Pomponio, BSc<sup>1,21</sup>, Haochang Shou, PhD<sup>3,1</sup>, Jimit Doshi, MSc<sup>1,21</sup>, Elizabeth Mamourian, BA<sup>1,21</sup>, Guray Erus, PhD<sup>1,21</sup>, Ilya Nasrallah, MD, PhD<sup>21,1</sup>, Lenore J Launer, PhD<sup>4</sup>, Tanweer Rashid, PhD<sup>1,21</sup>, Murat Bilgel, PhD<sup>5</sup>, Yong Fan, PhD<sup>1,21</sup>, Jon B. Toledo, MD, PhD<sup>6,7</sup>, Kristine Yaffe, MD<sup>8</sup>, Aristeidis Sotiras, PhD<sup>1,9</sup>, Dhivya Srinivasan, MSc<sup>1,21</sup>, Mark Espeland, PhD<sup>10</sup>, Colin Masters, MD<sup>11</sup>, Paul Maruff, PhD<sup>11</sup>, Jurgen Fripp, PhD<sup>12</sup>, Henry Völzk, MD<sup>13</sup>, Sterling C. Johnson, PhD<sup>14</sup>, John C. Morris, MD<sup>15</sup>, Marilyn S. Albert, PhD<sup>16</sup>, Michael I Miller, PhD<sup>17</sup>, R. Nick Bryan, MD<sup>18</sup>, Hans J. Grabe, MD<sup>19,20</sup>, Susan M. Resnick, PhD<sup>5</sup>, David A. Wolk, MD<sup>2,1</sup>, Christos Davatzikos, PhD<sup>1,21,\*,#</sup>

<sup>1</sup>Center for Biomedical Image Computing and Analytics, University of Pennsylvania, USA

<sup>2</sup>Department of Neurology and Penn Memory Center, University of Pennsylvania, USA

<sup>3</sup>Department of Biostatistics, Epidemiology and Informatics, University of Pennsylvania, USA

<sup>4</sup>Laboratory of Epidemiology and Population Sciences, National Institute on Aging, USA

<sup>5</sup>Laboratory of Behavioral Neuroscience, National Institute on Aging, Baltimore, USA

<sup>6</sup>Department of Pathology and Laboratory Medicine, Institute on Aging, Center for Neurodegenerative Disease Research, University of Pennsylvania School of Medicine, Philadelphia, PA, USA

<sup>7</sup>Stanley Appel Department of Neurology, Houston Methodist Hospital, Houston, TX, USA

<sup>8</sup>Departments of Neurology, Psychiatry and Epidemiology and Biostatistics, University of California San Francisco, San Francisco, California, USA

<sup>9</sup>Department of Radiology, Washington University in St. Louis, St. Louis, MO

<sup>10</sup>Department of Biostatistics and Data Science, Wake Forest School of Medicine, Winston-Salem, North Carolina

\*Corresponding authors Mohamad Habes, habesm@upenn.edu, Christos Davatzikos, christos.davatzikos@penmedicine.upenn.edu, 3700 Hamilton walk, Richards Building, 7<sup>th</sup> floor, Center for Biomedical Image Computing Analytics, University of Pennsylvania, 19104 Philadelphia, USA, <https://www.med.upenn.edu/cbica/>.

#for the iSTAGING consortium, the Preclinical AD consortium, the ADNI, and the CARDIA studies.

Authors' contributions

study design (MH, CD); statistical analysis (MH,RP,HS,IN,GE,LL,JT,NB,SR,DW,CD); data collection and processing (MH,JD,RP,EM,GE,IN, MB, YF,KY,AS,DS,ME,CM,PM,JF,HV,SJ, JM,MA,MM,NB,HG,SR, RNB, DW,CD); figure generation (MH,RP,EM,TR); literature search (MH,RP,EM); manuscript writing (MH); manuscript critical revision and submission approval (MH,RP,HS,JD,EM,GE,IN,LL,TR,MB, YF, JT, KY, AS, DS, ME, CM, PM, JF, HV, SJ, JM, MA, MM, NB, HG, SR, DW, CD)

Conflict of interest statements

None

<sup>11</sup>Florey Institute of Neuroscience and Mental Health, University of Melbourne, Melbourne, Australia

<sup>12</sup>CSIRO Health and Biosecurity, Australian e-Health Research Centre CSIRO, Australia

<sup>13</sup>Institute for Community Medicine, University of Greifswald, Germany

<sup>14</sup>Wisconsin Alzheimer's Institute, University of Wisconsin School of Medicine and Public Health, Madison, Wisconsin

<sup>15</sup>Department of Neurology, Washington University in St. Louis, St. Louis, MO

<sup>16</sup>Department of Neurology, Johns Hopkins University School of Medicine

<sup>17</sup>Department of Biomedical Engineering, Johns Hopkins University

<sup>18</sup>Department of Diagnostic Medicine, University of Texas, Austin; Austin, TX

<sup>19</sup>Department of Psychiatry and Psychotherapy, University of Greifswald, Germany

<sup>20</sup>German Center for Neurodegenerative Diseases (DZNE), Rostock/Greifswald, Germany

<sup>21</sup>Department of Radiology, University of Pennsylvania, USA

## Abstract

**INTRODUCTION:** Relationships between brain atrophy patterns of typical aging and Alzheimer's Disease (AD), white matter disease, cognition, and AD neuropathology were investigated via machine-learning in a large harmonized MRI database (11 studies; 10,216 subjects).

**METHODS:** Three brain signatures were calculated: Brain-Age, AD-like neurodegeneration, and white matter hyperintensities (WMH). Brain-charts measured and displayed these signatures' relationships to cognition, and molecular biomarkers of AD.

**RESULTS:** WMH were associated with advanced brain aging, AD-like atrophy, poorer cognition, and AD neuropathology in MCI/AD and cognitively normal (CN) subjects. High WMH volume was associated with Brain-Aging and cognitive decline occurring in a ~ten year-period in CN. WMH were associated with doubling  $\beta$ -amyloid positivity likelihood after age 65. Brain aging, AD-like atrophy, and WMH were better predictors of cognition than chronological age in MCI/AD.

**DISCUSSION:** A brain-chart quantifying brain aging trajectories was established, enabling the systematic evaluation of individuals' brain aging patterns relative to this large consortium.

## 1 Introduction

Aging is a complex and multi-factorial process, heterogeneously affecting brain structures<sup>1-3</sup>, due to multiple potential age-associated pathological processes superimposed upon changes related to the 'normal' brain aging that occur in the absence of concurrent pathology. While a variety of neurodegenerative conditions associated with deposition of abnormal protein deposits in the brain, such as Alzheimer's disease (AD), increase in prevalence with age and cause neuronal injury and loss, aging itself appears to be linked to

synaptic and neuropil loss in the absence of a proteinopathy<sup>4</sup>. Brain aging in the absence of known co-pathology appears to be associated with gray matter loss using MRI and can be quantified via pattern analytic methods as a measure of “brain age”, which is somewhat separable from but overlapping with patterns of atrophy associated with neurodegenerative conditions<sup>5–10</sup>. Evidence from several studies shows that multiple risk factors may accelerate the brain aging process<sup>5,11</sup>, functionally manifested by an acceleration in cognitive decline. Brain aging and neurodegenerative atrophy have been linked to cognitive impairment affecting memory and executive function, however, each may differentially affect various cognitive domains. For example, typical brain aging and small vessel ischemic disease have been linked to deterioration of executive function<sup>12</sup> and working memory<sup>13</sup>. AD, which is associated with abnormal deposition of tau in neurofibrillary tangles (NFTs) and  $\beta$ -amyloid in neuritic plaques, usually results in an amnesic-predominant, multi-domain syndrome.

Recent advances in machine learning and neuroimaging have enabled the development of imaging markers that provide a summary measure of deviation of an individual’s brain structure or function from typical brain aging trajectories. Deviations from such models reflect biological processes that may reflect disease or resilience to age-associated conditions. Patterns of brain change across multiple dimensions, such as brain aging, white matter disease burden and neurodegenerative signatures, capture heterogeneity across individuals, leading to a multi-dimensional conceptualization of aging related disorders where every individual shows unique patterns of brain alterations.

Structural magnetic resonance imaging (MRI) captures patterns of neurodegeneration and small vessel ischemic disease. Although there is now considerable information on brain aging using morphometric MRI methods<sup>5–10,14,15</sup>, the complexity and heterogeneity of factors affecting brain aging necessitate much larger and diverse cohorts. Critically, clinical adoption of imaging biomarkers requires stability and generalization across populations and scanner characteristics. Larger, diverse cohorts can be assembled by pooling together and harmonizing data from multiple studies to enable detection of complex associations between brain structure, neuropathology, and cognition using advanced quantitative metrics, although harmonization must be carefully performed to minimize removal of clinically relevant information. The current study overcomes previous limitations by pooling and harmonizing data from 11 cohorts with 10,216 brain MRIs to develop a unique resource defining brain normative curves of brain aging throughout the AD continuum, termed the Brain Chart.

The Brain Chart is developed using advanced image-analysis, machine-learning-based imaging indices, and the large harmonized sample. Importantly, it provides the potential for personalized quantification of white matter disease and patterns of brain atrophy in brain aging and AD, allowing investigation of the clinical utility of these biomarkers. We modeled structural MRI brain changes using the following summary signatures: i) the SPARE-BA index (MRI brain age), which measures “typical” age-related brain atrophy patterns derived from cognitively normal adults across the lifespan<sup>5,6</sup>, ii) the SPARE-AD index<sup>5,16</sup>, a relatively specific imaging signature of AD-like brain atrophy, which has also been found to predict progression from normal cognition to MCI<sup>16</sup>; and iii) total white matter hyperintensity (WMH) volume, a measure of white matter disease<sup>1</sup>.

These measurements provide individualized metrics of three types of age-related brain changes and can be used to determine the relationships between these changes as well as to chronological age and cognition. We hypothesized that these Brain Chart indices derived using machine learning and harmonized data from a large, diverse consortium of studies pooled. Together will demonstrate associations with cognitive performance. In addition, we hypothesized that cerebrovascular disease captured by WMH volume would be associated with worsened SPARE-BA and worsened cognitive testing. Further, given prior work linking cerebrovascular disease with AD, we hypothesized both WMH volume and SPARE-AD index would predict the presence of cerebral amyloid deposition. We anticipated these results would be present in both cognitively normal adults and those with cognitive impairment.

## 2 Materials and Methods

### 2.1 Participants in iSTAGING

We included 10,216 participants encompassing a wide age range (22–90 years) from the Imaging-based coordinate SysTem for AGing and NeurodeGenerative diseases (iSTAGING) consortium, with cognitively healthy individuals (n=8,284) and patients with mild cognitive impairment (MCI) and Alzheimer’s disease (AD) (n=1,932) to build the Brain Chart. The iSTAGING consortium included data from the following cohorts: The Alzheimer’s Disease Neuroimaging Initiative (ADNI 1 and ADNI 2), The University of Pennsylvania Aging Brain Cohort (Penn-ABC), The University of Pennsylvania Memory Center cohort (Penn-PMC), The Study of Health in Pomerania (SHIP), The UK Biobank (UKBIOBANK), The Baltimore Longitudinal Study of Aging (BLSA), The Australian Imaging, Biomarker, and Lifestyle (AIBL) Study, The Coronary Artery Risk Development in Young Adults (CARDIA) Study, The Adult Children Study at Washington University (ACS), The Biomarkers of Cognitive Decline Among Normal Individuals in the Johns Hopkins University (BIOCARD) and The Wisconsin Registry for Alzheimer’s Prevention (WRAP). Fig. 1 shows a flowchart for the included subjects. The supervisory committee of each cohort approved its inclusion in this study, and this study was approved by the institutional review board of the University of Pennsylvania.

**2.1.1 Clinical assessment and cognitive tests in iSTAGING**—iSTAGING cohorts included a diverse and heterogeneous set of clinical data. Our main objective in this analysis was to collect a common subset of brain aging-related risk factors<sup>5</sup> and neuropsychological tests, while also maximizing the possible sample sizes from different cohorts. With this objective in mind, we included cognitive testing and focused on tests of executive function and memory. Selection of cognitive testing varied widely across the different cohorts. We selected the Trail Making Test (TMT) considering the difference between the sub-scores (TMT-B – TMT-A) as a measure of executive function (n= 4,757). We selected the California Verbal Learning Test long-delay free recall (CVLT-long) as the most sensitive measure for memory function (n= 1128) across cohorts in the cognitively normal group; CVLT was not widely available across the AD/MCI groups so mini-mental status examination (MMSE) was used as a measure of cognitive impairment in these participants

(n= 1,918). Details of the neuropsychological tests for the individual participating cohorts are given in Supplement S.1 and Supplementary Tables 3 and 4.

**2.1.2  $\beta$ -amyloid and tau status**—In contrast to other clinical variables, measurements of A $\beta$  and tau protein, the pathologic hallmarks of AD, were only available for a relatively small set of participants (Supplementary Tables 3 and 4). We considered A $\beta$  status as a binary variable (negative or positive), as derived from CSF or PET (n=1,382). Additionally, we considered phosphorylated tau assessed from CSF, as a tau measure that is more specific to AD (n=1,215). We used previously established thresholds for amyloid and tau positivity; more detail on molecular markers of AD pathology in iSTAGING can be found in Supplementary Table 1 and Section S.2.

## 2.2 Imaging protocols and image pre-processing

We chose a sample that varied across MRI acquisition protocols from 11 cohorts in iSTAGING so that results would be more generalizable across populations. Imaging parameters for each of the individual studies of iSTAGING are described in Supplementary Table 2. We used a standardized and fully automated processing pipeline to derive final imaging variables from this highly heterogeneous data set. Preprocessing included bias correction<sup>17</sup> and multi-atlas skull stripping on the T1-weighted images<sup>18</sup>. A robust multi-atlas label fusion-based method was applied for segmentation of the brain into a set of anatomic regions of interest (ROIs)<sup>19</sup>. ROI volumes were quantified for all iSTAGING participants with T1 images (n=10,216). WMH segmentation was performed using a deep learning-based method that operated on raw FLAIR and T1-weighted images<sup>20</sup> (n=8,596). The details of the processing algorithms are given in the Supplementary S.3.

## 2.3 Harmonization of ROI volumes

Removal of cohort-related effects, such as protocol-specific variability, is critical for pooling such diverse data together for analysis. Imaging measures were harmonized using regression-based methods that removed cohort effects for each measure<sup>21</sup>. For each ROI Volume, a Location/Scale adjustment is made for each cohort<sup>21,22</sup>. The location adjustment corrects for mean shifts across sites, and the scale adjustment corrects for differences in variance across sites. Our harmonization method models ROI Volumes as a nonlinear function of age and sex, using cubic splines; adjusting only Location/Scale effects and thereby preserving age and sex differences across sites. We perform the harmonization exclusively using cognitively healthy subjects from each dataset, and then apply the same correction towards the entire dataset. This procedure is based on the method described in detail by Pomponio et al<sup>21</sup> (Supplementary Section S3).

## 2.4 Dimensions of the Brain Chart coordinate system

We projected complex imaging data into a lower-dimensional coordinate system that reflects important different aspects of brain structural changes related to aging and disease using three summary indices. These indices have been previously validated and reflect patterns of brain changes measuring predicted brain age (SPARE-BA)<sup>5,6</sup>, AD-like atrophy patterns captured by SPARE-AD<sup>23,5</sup>, and white matter disease as measured by WMH volume. The SPARE indices were derived from the harmonized ROI using machine learning methods.

While we calculated the SPARE-BA index for the entire sample, we calculated SPARE-AD using the amyloid positive AD participants and age-matched amyloid negative cognitively normal participants, resulting in using participants aged >55 years. Higher SPARE-BA values indicate greater age-related atrophy compared to normative trends of age-related changes in brain structure. Higher SPARE-AD scores indicate more AD-related atrophy, while lower and negative scores indicate more normal appearance. Total WMH volume was calculated from deep learning-based segmented images<sup>20</sup>. More detail on these indices is provided in the Supplementary Section S.3.

## 2.5 Brain Chart in Aging

We investigated associations between Brain Chart imaging dimensions and multiple other variables. Since we can only display at most three dimensions at a time, we demonstrate associations of interest via projection charts. Each of these charts represents in the x-axis the chronological age of the subject and in the y-axis one of the iSTAGING dimensions. The associations with a third target variable, e.g., cognitive test results, are shown using colormaps, with red/blue indicating higher/lower values. To further assist in the interpretation of these maps, we display isocontours, which are curves of constant value for the third variable overlaid over the colormaps. As an example, consider an isocontour of a memory score in a SPARE-BA vs. age plot. This isocontour indicates (age vs. SPARE-BA) measurements from all individuals having the same level of memory performance. Vertical isocontours in such a map would indicate that SPARE-BA has no effect on memory for a given age. Conversely, horizontal isocontours would indicate that SPARE-BA, and not age, is more predictive of memory performance. More on the implementation of the brain aging charts can be found in the supplementary section S4. The brain aging charts code can be downloaded<sup>24</sup> and the models used in this work can be also accessed as a reference in an online stand-alone application, in which independent dimensions of interest could also be plotted<sup>25</sup>.

## 2.6 Statistical analysis

We studied patterns of advanced brain aging and AD-like atrophy independently in two age categories: middle age (40–65 years old) and old age (>65 years old). In each age category, we modeled the relationship between age as the independent variable and SPARE-AD as the dependent variable in a quantile regression approach, to identify high SPARE-AD (75<sup>th</sup> percentile) and low SPARE-AD (25<sup>th</sup> percentile) individuals. We identified “advanced brain aging” versus “resilient to brain aging” subjects as those with SPARE-BA scores 5 years higher than their actual age and those with SPARE-BA scores 5 years lower than their actual age, respectively. We applied Student’s t-test on brain ROIs between groups and only results that survived Bonferroni correction were considered significant. We computed age-specific regional patterns of WMH load by averaging WMH maps aligned to a common atlas space in 5 different age categories from 5<sup>th</sup> decade to 9<sup>th</sup> decade.

In order to estimate isocontours in the Brain-Charts, we fit a Generalized Additive Model<sup>26</sup> with the age and one of the iSTAGING dimensions used as the predictors, and the single selected outcome variable, e.g. a specific cognitive test score or marker of AD pathology, as the response. All models included a term for the parent study. Models that included

cognitive testing as an outcome variable were also corrected for education. We performed a likelihood ratio test for model comparison between a model with age as the single predictor and a model with age and an additional predictor. All resulting p-values were corrected using the Benjamini-Hochberg approach controlling 5% false-discovery rate (FDR) and those  $<0.05$  were reported as significant. We calculated the 95% confidence bands of each isocontour to ensure robustness in the level of the isocontour using a bootstrapping approach and plotted only significant isocontours, for which the confidence bands do not overlap (Supplementary S.4). Due to skewness in the raw data, TMT score, the difference between TMT-B and TMT-A, and WMH were cube-root transformed to achieve normal distribution. Statistical analyses were performed using R software v3.3.

### 3 Results

#### 3.1 Subjects

We included 10,216 participants (age 22–90 years) from iSTAGING. Cognitively normal (CN) individuals ( $n=8,284$ ) had a mean (SD) age of 60.5 (13.1) years; 54.5% were female. Among the patients with MCI or AD ( $n=1,932$ ), the mean (SD) age was 74.3 (7.7) years; 47.2% were female. A detailed description of the CN cohorts is presented in Supplementary Table 3. The description of MCI and AD cohorts is given in Supplementary Table 4.

#### 3.2 SPARE-BA, SPARE-AD and white matter disease dimensions in CN

Fig. 2.A shows the SPARE-BA scores calculated for the iSTAGING CN sample. Neuroanatomical pattern of advanced (SPARE-BA 5+ years older) vs. resilient (SPARE-BA 5+ years younger) brain aging suggests that advanced brain aging (overall a  $>10$ -year SPARE-BA difference) was associated with lower gray matter volumes that were widespread but most pronounced in the frontal operculum, superior temporal, insular, frontal and inferior parietal cortex, in addition to enlargement of the ventricles (Fig. 2.B, Supplementary Fig.1 and Tables 5–6). While the spatial pattern was similar, those with older chronologic age (65–90 years) had smaller effect sizes than middle age (40–65 years) groups (Fig. 2.B, Supplementary Fig.1 and Supplementary Tables 5–6).

SPARE-AD scores of CN subjects in iSTAGING are shown in Fig. 2.C. SPARE-AD values displayed predominantly negative values, and a consistently increasing trend with age. Importantly, at middle age, high SPARE-AD subjects showed a more notable deviation from the norm compared to older ages. AD-like atrophy showed a more specific regional pattern compared to SPARE-BA (Fig. 2.D). Lower gray matter volumes associated with higher SPARE-AD were most pronounced in the hippocampus, amygdala, entorhinal cortex and inferior temporal cortex. Effect sizes were smaller in the older age ( $>65$  years) than in the middle age (40–65 years) group (Fig. 2.D, Supplementary Fig.1 and Supplementary Tables 7–8).

In CN individuals, WMH started to appear after the 5<sup>th</sup> decade of life with a highly non-linear trend of increase in WMH volume with age (Fig. 2.E). WMH showed a regional pattern of burden that becomes apparent in periventricular areas around the 6<sup>th</sup> decade of age



and that increases with older age, both in terms of the spatial extent and the frequency of occurrence across subjects (Fig. 2.F).

### 3.3 Brain Charts of BA, AD-like atrophy and WMH in CN subjects

Associations between the iSTAGING imaging dimensions and other variables were evaluated using the Brain Chart projections. Advanced brain aging was associated with lower executive function (Fig. 3.A) but not with memory function (Supplementary Fig. 2). AD-like atrophy was associated with both executive and memory functions (Fig. 3.B–C) after age 65 years.

Higher WMH burden was associated with advanced SPARE-BA (Fig. 4.A). This association was modulated by age: among middle-aged individuals, higher WMH volume had a stronger association with advanced brain aging (i.e., older SPARE-BA than actual age) as compared to individuals at older ages (>80 years). WMH were also associated with SPARE-AD after age 65 (Fig. 4.B), an association which persisted after adjustment for SPARE-BA in the sensitivity analysis (Supplementary Fig. 3). Increasing WMH was associated with decline in both executive function in participants over age 40 (Fig. 4.C) and memory in participants over age 50 (Fig. 4.D). Higher total WMH volume after age 55 was associated with a higher probability of being positive for cerebral  $\beta$ -amyloid (Fig. 4.E) but not for tau (Supplementary Fig. 4).

### 3.4 Brain Charts in MCI and AD patients

Contrary to the findings observed in CN where chronological age had stronger effects, executive function and memory were primarily associated with SPARE-BA and SPARE-AD, depicted by the relatively horizontal isocontours in Fig. 5.A–D. In other words, Brain age (SPARE-BA) is a better predictor of cognitive decline in executive function and memory compared to chronological age. Notably, these associations were stronger in MCI/AD compared to CN (as measured by the higher range and steeper isocontours). WMH regional distribution was more extensive; burden was higher in the MCI/AD population compared to the CN population (Fig. 6.A, compare to Fig 2.F). Figures 5.E–F and Fig. 6.B–C show the associations between WMH, advanced brain aging, AD-like atrophy, and executive function and memory in the MCI and AD stages. Importantly, Fig. 6.B indicates that the association of WMH with advanced aging is more pronounced at relatively younger ages. The effect of WMH on executive function is also more pronounced at younger ages (relatively horizontal isocontours in Fig. 5.E), whereas at older ages, both WMH and age were equal contributors to diminished executive function. Finally, similar to CN individuals, WMH showed a significant relationship with the presence of amyloid pathology in MCI and AD (Fig. 6.D). At the middle ages, WMH volume but not chronological age was associated with increased prevalence of amyloid positivity, but at older ages (>80 years-old) the association between WMH volume and amyloid positivity was almost not present.

## 4 Discussion

We established a dimensional and quantitative summarization of brain MRI scans, the Brain Chart of Aging, from a large, harmonized, multi-site consortium, using machine learning

methods. We found important associations between imaging signatures of the Brain Chart, cognition and AD neuropathology. The large sample along with the harmonization methodology helped us construct robust neuroimaging markers of aging and early AD from heterogeneous data, which better reflect diversity across people, clinical centers, and MRI protocols. The three main axes of the Brain Chart were a brain aging index, an AD-like atrophy index, and a measure of white matter disease captured with WMH. Higher brain age was associated with reduced executive function, and higher SPARE-AD and WMH were both associated with lower executive and memory function in the cognitively normal population. Our results also demonstrate that WMH are associated with advanced brain aging, AD-like atrophy patterns, cognitive decline, and presence of cerebral  $\beta$ -amyloid deposition. These associations also persisted in MCI and AD patients, further suggesting a potential role of WMH in disease progression.

This study is among the first to develop neuroimaging signatures across multiple cohorts using machine learning methods, and produced imaging signatures that could provide individualized prognostic information. A recent review showed intensive research in the use of machine learning and neuroimaging for building signatures for neuropsychiatric diseases with more than 450 models published to date<sup>27</sup>. However, few of these signatures have had rigorous cross-validation in independent samples. In this work, we provide further validation of the utility of SPARE-AD<sup>27</sup> and of SPARE-BA.

#### 4.1 Advanced brain aging and cognitive decline

In a prior study, we showed considerable overlap between advanced brain aging patterns of atrophy and those related to AD<sup>5</sup>, but the effect of advanced brain aging on cognitive decline was not apparent due to limited cognitive testing. In the current cross-sectional study, we demonstrated that advanced brain aging patterns in CN were associated with lower executive function but not worse memory performance. In contrast, higher SPARE-AD, characterized by a pattern showing greater atrophy in temporal lobe regions, was associated with both executive function and memory. These results support prevailing hypotheses that different regional atrophy patterns are associated with different cognitive impairment profiles, and importantly show that the Brain Chart machine learning indices are sensitive for different cognitive outcomes. Furthermore, AD is heterogeneous in its phenotype and pattern of neurodegeneration with, for example, relative dysexecutive versus amnesic presentations<sup>28,29</sup>. Advanced brain aging may contribute to dysexecutive patterns of cognitive impairment in some patients.

The observation that brain age, as well as other Brain Chart dimensions, show stronger associations with cognitive scores than chronologic age fits with the concept that certain, apparently age-associated, phenomena may better be characterized as related to changes that occur preceding a transition to dementia or at the end of life, termed terminal decline<sup>30</sup>. Prospectively, these transition events are unknown and such data is not available for this cohort, but the accumulation of adverse changes in brain age, SPARE-AD, or WMH volume, conceptually quantify progression towards these events.

## 4.2 WMH and the association with SPARE-AD and SPARE-BA

WMH are established biomarker of small vessel ischemic injury in the brain, strongly associated with vascular risk factors, specifically hypertension, and related to vascular contributions to cognitive impairment and dementia (VCID). Several mechanisms have been proposed to explain the association between WMH and gray matter atrophy, such as ischemic damage<sup>31</sup> or Wallerian degeneration<sup>32</sup>. Vascular risk factors have been linked to development of AD neuropathology and advanced brain aging<sup>33,34</sup>. However, it is unclear whether the effects of VCID and AD are merely additive or whether they are synergistic. The association of WMH to AD-like atrophy observed in this study has been previously observed, albeit often in single cohorts<sup>1,6</sup>. In this study, the association between WMH and SPARE-BA was relatively more pronounced at younger than in older ages, both in CN individuals and in MCI and AD. A couple factors likely underlie this finding. First, younger and overall healthier brains are relatively more homogeneous in brain structure in the CN group, so presence of WMH-related atrophy can be detected even if relatively mild. Second, vascular disease, while present in a minority, is one of the few processes active at younger ages; the widespread prevalence of WMH and heterogeneous presence of other neuropathologic processes later in life diminishes the relative influence of WMH on brain aging. This finding underlines the importance of modifying vascular risk factors at middle-age<sup>11</sup>.

## 4.3 WMH and the association with AD pathology

Our observation of associations between WMH and increased levels of AD pathology markers at any given age add to recent body of literature<sup>35,36</sup> and has important implications. Possibilities for the link between WMH and AD pathology include i) Wallerian degeneration secondary to neurodegenerative changes, ii) ischemic injury to axons, manifested as white matter changes, which may lead to tangle formation and neuronal degeneration<sup>32</sup>, iii) demyelination, which could be present in AD and lead to the appearance of WMH<sup>37</sup>. However, WMH were associated with approximately double the likelihood of  $\beta$ -amyloid positivity throughout all ages in the CN cohort. While this result is intriguing and suggests the possibility that prevention of small vessel ischemic disease might delay AD pathology and brain aging, the current study is unable to elucidate whether this relationship is causal or results from another latent neuropathologic process that leads to both WMH and  $\beta$ -amyloid deposition and might be a primary treatment target in AD. This observation may help enrich clinical trials for  $\beta$ -amyloid positive individuals, as MRI is commonly obtained in AD clinical trials.

## 4.4 WMH and the association with cognitive function

Our data demonstrate that the association between WMH and cognitive decline can start as early as in the age of 40, more than two decades before the age at which the prevalence of AD dementia reaches 1%. This finding, especially in conjunction with the relationship between WMH and AD pathology markers, further demonstrates the potential role of WMH as an early contributor to AD. Previous work showed that WMH were associated with declining executive function<sup>38</sup> and that vascular risk factors were associated with smaller prefrontal volumes<sup>39</sup>. The anterior temporal lobe has dense connectivity with several

sensory modalities, e.g., white matter tracts have been observed between the anterior temporal lobe and the frontal lobe via the uncinate fasciculate<sup>40</sup>, which might explain the association with cognitive decline in memory and executive functions.

The emphasis in this paper was on cross-sectional relationships between imaging signatures and other variables, including cognition. However, one of the main goals of this work is to develop prognostic markers, based on the Brain Chart's coordinates, i.e. expression of these imaging signatures. Application of this Brain Chart to longitudinal studies, including the ones already part of iSTAGING<sup>2,41-43</sup> will allow us to construct personalized predictions of an individual's brain aging trajectory, based on her/his Brain Chart coordinates. In this study we have established different associations of the Brain Chart coordinates, suggesting that they may be useful to predict future cognitive decline on an individual basis.

This study has several strengths including the large sample size, diverse harmonized populations with rich phenotyping and the use of machine learning signatures as well as automated pipelines and advanced statistics to build highly quantitative brain charts enabling prediction at an individual level. However, this study also has limitations. i) We did not include serial MRI to study longitudinal effects, which requires additional effort in harmonization. ii) Our analysis did not include other measures of small vessel disease such as infarcts and periventricular spaces assessment, and those should be considered in future research. iii) MCI diagnosis was not necessarily due to Alzheimer's disease, and we did not exclude subjects who developed mild cognitive impairment without ever progressing to Alzheimer's disease. For this study, we included all subjects with cognitive decline, whether the disease progressed beyond MCI or not. We acknowledge that this grouping of MCI participants, while common, can decrease power to detect early AD-related changes. iv) The heterogeneity in sampling strategies and exclusion criteria of each study might still pose difficulties in generalizing our study findings without clearly defining a reference population. Hence our results are generalizable with respect to our pooled samples, which as far as we know, is one of the largest MRI databases available. v) Furthermore, while our consortium is large, some important biomarkers such as  $\beta$ -amyloid or tau positivity status were less available across cohorts, decreasing our statistical power for these markers. vi) While the three Brain Chart coordinates used in this study provide insight into understanding some of the most common brain age-related processes, they do not specifically account for other pathologies in the brain such as Limbic-predominant age-related TDP-43 encephalopathy (LATE) pathology, which were likely present in varying, low frequencies in this large sample. Contributions of other pathologies could be added with incorporation of appropriate data sets in the future. vii) Further, SPARE-BA and WMH volumes in particular are not intrinsically disease-specific, but rather capture contributions from a number of potential co-pathologies. This can increase the applicability of these indices, but greater disease specificity could be obtained as additional data allows for further tailoring of these measurements and development of additional Brain Chart dimensions.

## 5 Conclusion

A Brain Chart derived from a large, harmonized, multi-site sample is established as a means to understand relationships between brain aging, cognition, and AD neuropathology.

Machine-learning-based methods are used to derive three comprehensive, yet complementary, imaging signatures of typical brain aging, AD neurodegeneration, and white matter disease, reflecting the effects of underlying neuropathologic processes on brain structure. By plotting these dimensions, which have previously demonstrated prognostic value<sup>5,6,8,12,16,35,36</sup>, onto a standardized coordinate system, one can derive a systematic and quantitative way to assess an individual's brain health. Our results utilizing this Brain Chart revealed many relationships. In particular, one of the most conclusive findings of our study was the importance of white matter disease, which was associated with worse cognitive function, advanced brain aging, increased expression of AD-patterns of atrophy and  $\beta$ -amyloid positivity. Our results do not necessarily imply causality in the aforementioned relationships, but rather demonstrate a very strong statistical association, which suggests that preventive strategies against white matter disease might delay cognitive aging. Recent evidence from interventional studies supports this hypothesis<sup>44</sup>.

## Supplementary Material

Refer to Web version on PubMed Central for supplementary material.

## Acknowledgments

We would like to thank the anonymous reviewers for their constructive comments, that improved the quality of this work substantially. For further acknowledgments please attached document

Role of funding source

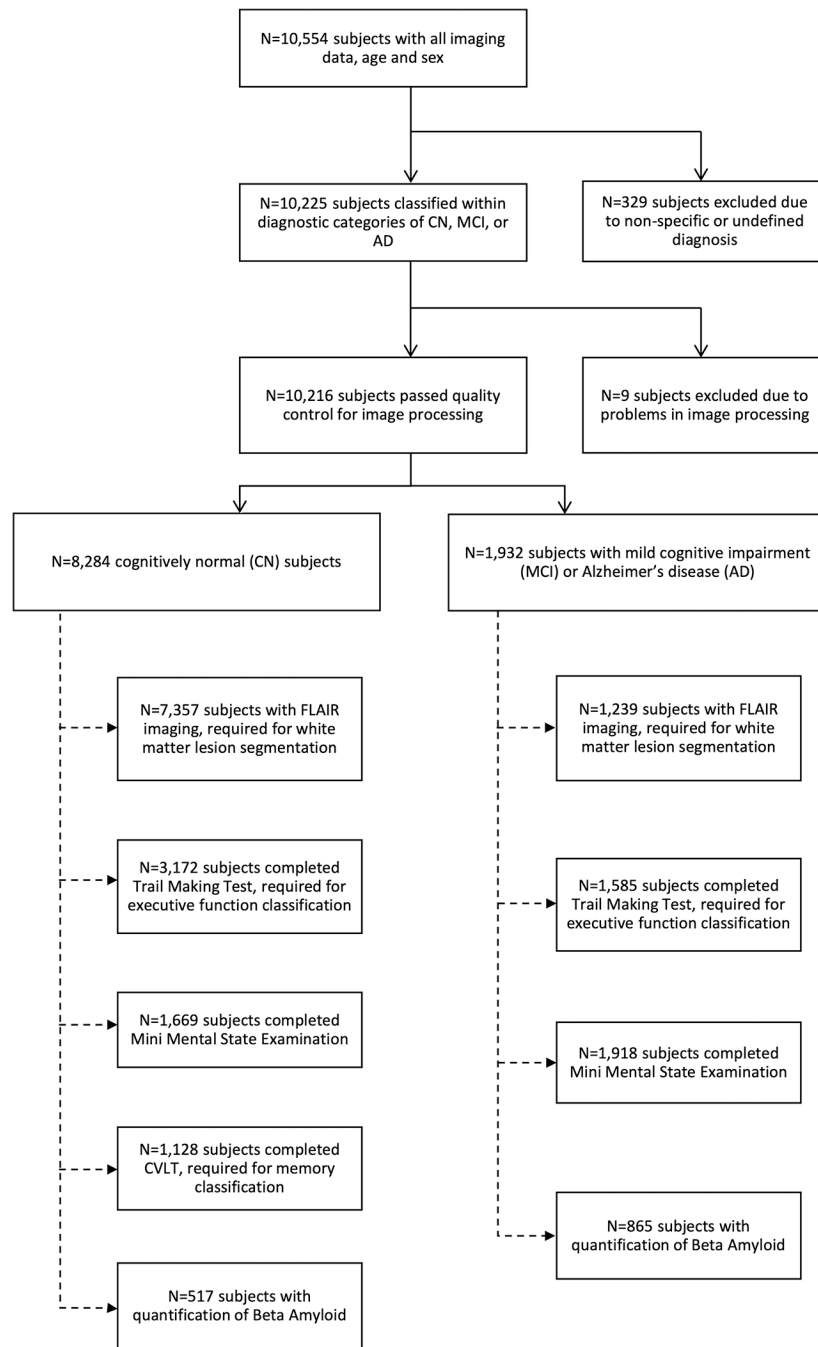
R01 AG054409, HHSN271201600059C, Intramural Research Program of NIH. Funding agencies were not involved in writing or the decision to submit the publication

## References

1. Habes M, Erus G, Toledo JB, et al. White matter hyperintensities and imaging patterns of brain aging in the general population. *Brain*. 2016;139(Pt 4):1164–1179. doi:10.1093/brain/aww008 [PubMed: 26912649]
2. Resnick SM, Pham DL, Kraut MA, Zonderman AB, Davatzikos C. Longitudinal Magnetic Resonance Imaging Studies of Older Adults: A Shrinking Brain. *J Neurosci*. 2003;23(8):3295–3301. <http://www.jneurosci.org/content/23/8/3295.abstract> [PubMed: 12716936]
3. Raz N, Ghisletta P, Rodrigue KM, Kennedy KM, Lindenberger U. Trajectories of brain aging in middle-aged and older adults: regional and individual differences. *NeuroImage*. 2010;51(2):501–511. doi:10.1016/j.neuroimage.2010.03.020 [PubMed: 20298790]
4. Benavides-Piccione R, Feraud-Espinosa I, Robles V, Yuste R, DeFelipe J. Age-based comparison of human dendritic spine structure using complete three-dimensional reconstructions. *Cereb Cortex N Y N* 1991. 2013;23(8):1798–1810. doi:10.1093/cercor/bhs154
5. Habes M, Janowitz D, Erus G, et al. Advanced Brain Aging: relationship with epidemiologic and genetic risk factors, and overlap with Alzheimer disease atrophy patterns. *Transl Psychiatry*. 2016;6:e775. [PubMed: 27045845]
6. Eavani H, Habes M, Satterthwaite TD, et al. Heterogeneity of structural and functional imaging patterns of advanced brain aging revealed via machine learning methods. *Neurobiol Aging*. 2018;71:41–50. doi:10.1016/j.neurobiolaging.2018.06.013 [PubMed: 30077821]
7. Gaser C, Franke K, Klöppel S, Koutsouleris N, Sauer H, Initiative ADN. BrainAGE in Mild Cognitive Impaired Patients: Predicting the Conversion to Alzheimer's Disease. *PLoS ONE*. 2013;8(6):e67346. doi:10.1371/journal.pone.0067346 [PubMed: 23826273]

8. Cole JH, Franke K. Predicting Age Using Neuroimaging: Innovative Brain Ageing Biomarkers. *Trends Neurosci.* 2017;40(12):681–690. doi:10.1016/j.tins.2017.10.001 [PubMed: 29074032]
9. Wang J, Knol MJ, Tiulpin A, et al. Gray Matter Age Prediction as a Biomarker for Risk of Dementia. *Proc Natl Acad Sci U S A.* 2019;116(42):21213–21218. doi:10.1073/pnas.1902376116 [PubMed: 31575746]
10. Kaufmann T, van der Meer D, Doan NT, et al. Common brain disorders are associated with heritable patterns of apparent aging of the brain. *Nat Neurosci.* 2019;22(10):1617–1623. doi:10.1038/s41593-019-0471-7 [PubMed: 31551603]
11. Debette S, Seshadri S, Beiser A, et al. Midlife vascular risk factor exposure accelerates structural brain aging and cognitive decline. *Neurology.* 2011;77(5):461–468. doi:10.1212/WNL.0b013e318227b227 [PubMed: 21810696]
12. Habes M, Sotiras A, Erus G, et al. White matter lesions: Spatial heterogeneity, links to risk factors, cognition, genetics, and atrophy. *Neurology.* 2018;91(10):e964–e975. doi:10.1212/WNL.0000000000006116 [PubMed: 30076276]
13. Buckner RL. Memory and Executive Function in Aging and AD: Multiple Factors that Cause Decline and Reserve Factors that Compensate. *Neuron.* 2004;44(1):195–208. doi:10.1016/j.neuron.2004.09.006 [PubMed: 15450170]
14. Liem F, Varoquaux G, Kynast J, et al. Predicting brain-age from multimodal imaging data captures cognitive impairment. *NeuroImage.* 2017;148:179–188. doi:10.1016/j.neuroimage.2016.11.005 [PubMed: 27890805]
15. Franke K, Gaser C, Manor B, Novak V. Advanced BrainAGE in older adults with type 2 diabetes mellitus. *Front Aging Neurosci.* 2012;5. doi:10.3389/fnagi.2013.00090 [PubMed: 22539924]
16. Davatzikos C, Xu F, An Y, Fan Y, Resnick SM. Longitudinal progression of Alzheimer’s-like patterns of atrophy in normal older adults: the SPARE-AD index. *Brain.* 2009;132(8):2026–2035. doi:10.1093/brain/awp091 [PubMed: 19416949]
17. Tustison NJ, Avants BB, Cook PA, et al. N4ITK: Improved N3 Bias Correction. *Med Imaging IEEE Trans On.* 2010;29(6):1310–1320. doi:10.1109/TMI.2010.2046908
18. Doshi J, Erus G, Ou Y, Gaonkar B, Davatzikos C. Multi-Atlas Skull-Stripping. *Acad Radiol.* 2013;20(12):1566–1576. doi:10.1016/j.acra.2013.09.010 [PubMed: 24200484]
19. Doshi J, Erus G, Ou Y, et al. MUSE: Multi-atlas region Segmentation utilizing Ensembles of registration algorithms and parameters, and locally optimal atlas selection. *NeuroImage.* 2016;127:186–195. doi:10.1016/j.neuroimage.2015.11.073 [PubMed: 26679328]
20. Doshi J, Erus G, Habes M, Davatzikos C. DeepMRSeg: A convolutional deep neural network for anatomy and abnormality segmentation on MR images. *ArXiv Prepr ArXiv190702110.* Published online 2019.
21. Pomponio R, Erus G, Habes M, et al. Harmonization of large MRI datasets for the analysis of brain imaging patterns throughout the lifespan. *NeuroImage.* 2020;208:116450. doi:10.1016/j.neuroimage.2019.116450 [PubMed: 31821869]
22. Fortin J-P, Cullen N, Sheline YI, et al. Harmonization of cortical thickness measurements across scanners and sites. *NeuroImage.* 2018;167:104–120. doi:10.1016/j.neuroimage.2017.11.024 [PubMed: 29155184]
23. Da X, Toledo JB, Zee J, et al. Integration and relative value of biomarkers for prediction of MCI to AD progression: Spatial patterns of brain atrophy, cognitive scores, APOE genotype and CSF biomarkers. *NeuroImage Clin.* 2014;4(0):164–173. doi:10.1016/j.nicl.2013.11.010 [PubMed: 24371799]
24. Pomponio R, Habes M. gam-based isocontours visualization package. [https://github.com/rpomponio/gam\\_visualization](https://github.com/rpomponio/gam_visualization)
25. Pomponio R, Habes M. The brain aging charts: online app. Accessed July 7, 2020. [https://rpmponio.shinyapps.io/brain\\_aging\\_charts/](https://rpmponio.shinyapps.io/brain_aging_charts/)
26. Hastie T, Tibshirani R. Generalized additive models for medical research. *Stat Methods Med Res.* 1995;4(3):187–196. doi:10.1177/096228029500400302 [PubMed: 8548102]
27. Woo C-W, Chang LJ, Lindquist MA, Wager TD. Building better biomarkers: brain models in translational neuroimaging. *Nat Neurosci.* 2017;20(3):365–377. doi:10.1038/nn.4478 [PubMed: 28230847]

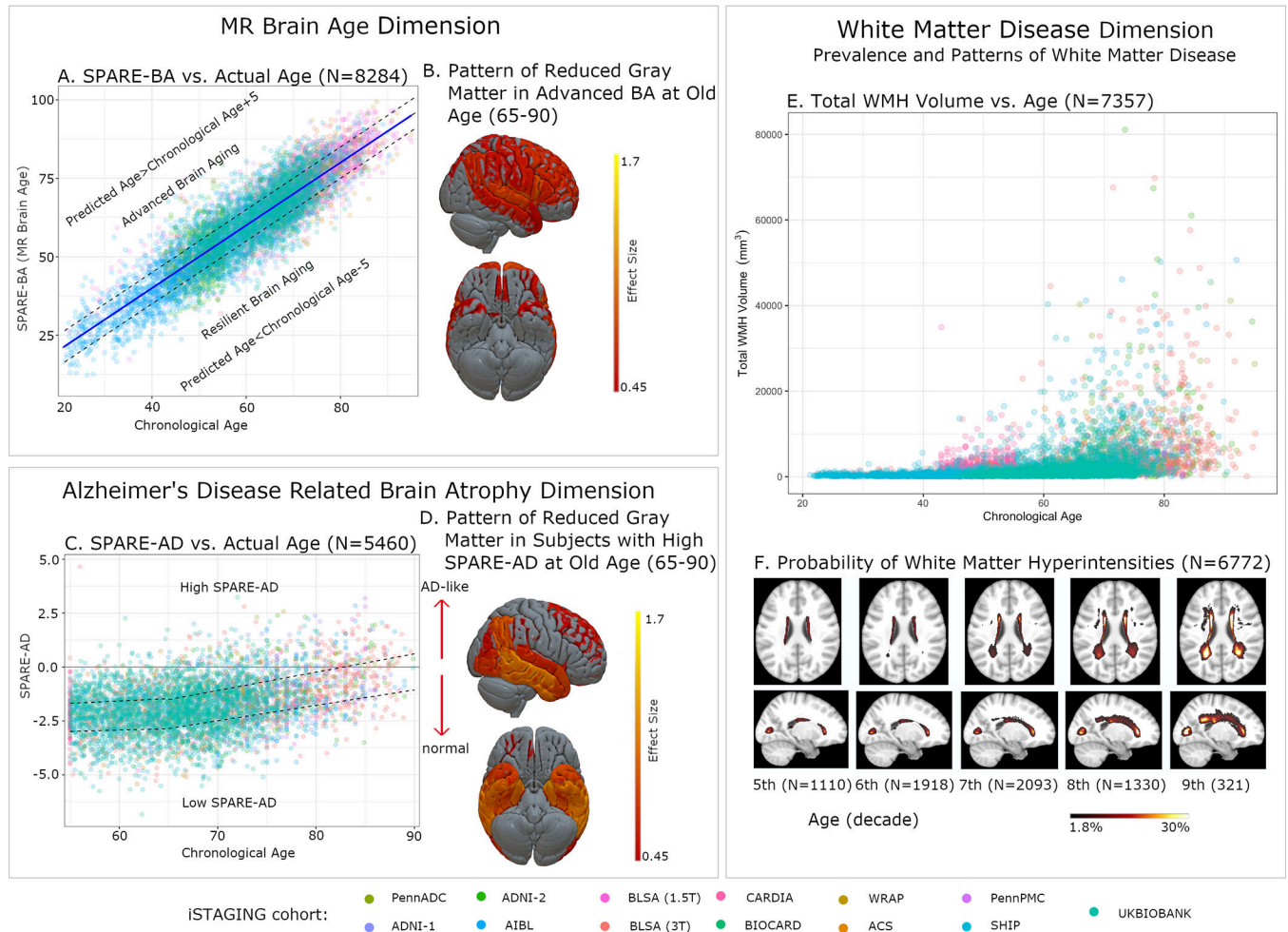
28. Dickerson BC, Wolk DA. Dysexecutive versus amnesic phenotypes of very mild Alzheimer's disease are associated with distinct clinical, genetic and cortical thinning characteristics. *J Neurol Neurosurg Psychiatry*. 2011;82(1):45–51. doi:10.1136/jnnp.2009.199505 [PubMed: 20562467]
29. Habes M, Grothe MJ, Tunc B, McMillan C, Wolk DA, Davatzikos C. Disentangling Heterogeneity in Alzheimer's Disease and Related Dementias Using Data-Driven Methods. *Biol Psychiatry*. Published online January 31, 2020. doi:10.1016/j.biopsych.2020.01.016
30. Bendayan R, Piccinin AM, Hofer SM, Cadar D, Johansson B, Muniz-Terrera G. Decline in Memory, Visuospatial Ability, and Crystallized Cognitive Abilities in Older Adults: Normative Aging or Terminal Decline? *J Aging Res*. 2017;2017:6210105. doi:10.1155/2017/6210105 [PubMed: 28634548]
31. Du A-T, Schuff N, Chao LL, et al. White matter lesions are associated with cortical atrophy more than entorhinal and hippocampal atrophy. *Neurobiol Aging*. 2005;26(4):553–559. doi:10.1016/j.neurobiolaging.2004.05.002 [PubMed: 15653183]
32. Erten-Lyons D, Woltjer R, Kaye J, et al. Neuropathologic basis of white matter hyperintensity accumulation with advanced age. *Neurology*. 2013;81(11):977–983. doi:10.1212/WNL.0b013e3182a43e45 [PubMed: 23935177]
33. Dai W, Lopez OL, Carmichael OT, Becker JT, Kuller LH, Gach HM. Abnormal Regional Cerebral Blood Flow in Cognitively Normal Elderly Subjects With Hypertension. *Stroke*. 2008;39(2):349–354. doi:10.1161/STROKEAHA.107.495457 [PubMed: 18174483]
34. Moran C, Phan TG, Chen J, et al. Brain Atrophy in Type 2 Diabetes: Regional distribution and influence on cognition. *Diabetes Care*. 2013;36(12):4036–4042. doi:10.2337/dc13-0143 [PubMed: 23939539]
35. Graff-Radford J, Arenaza-Urquijo EM, Knopman DS, et al. White matter hyperintensities: relationship to amyloid and tau burdens. *Brain J Neurol*. 2019;142(8):2483–2491. doi:10.1093/brain/awz162
36. Lee S, Viqar F, Zimmerman ME, et al. White matter hyperintensities are a core feature of Alzheimer's disease: Evidence from the dominantly inherited Alzheimer network. *Ann Neurol*. 2016;79(6):929–939. doi:10.1002/ana.24647 [PubMed: 27016429]
37. Ihara M, Polvikoski TM, Hall R, et al. Quantification of myelin loss in frontal lobe white matter in vascular dementia, Alzheimer's disease, and dementia with Lewy bodies. *Acta Neuropathol (Berl)*. 2010;119(5):579–589. doi:10.1007/s00401-009-0635-8 [PubMed: 20091409]
38. Tullberg M, Fletcher E, DeCarli C, et al. White matter lesions impair frontal lobe function regardless of their location. *Neurology*. 2004;63(2):246–253. [PubMed: 15277616]
39. Raz N, Lindenberger U, Ghisletta P, Rodrigue KM, Kennedy KM, Acker JD. Neuroanatomical correlates of fluid intelligence in healthy adults and persons with vascular risk factors. *Cereb Cortex N Y N 1991*. 2008;18(3):718–726. doi:10.1093/cercor/bhm108
40. Kubicki M, Westin C-F, Maier SE, et al. Uncinate fasciculus findings in schizophrenia: a magnetic resonance diffusion tensor imaging study. *Am J Psychiatry*. 2002;159(5):813–820. [PubMed: 11986136]
41. Johnson SC, Kosciak RL, Jonaitis EM, et al. The Wisconsin Registry for Alzheimer's Prevention: A review of findings and current directions. *Alzheimers Dement Amst Neth*. 2018;10:130–142. doi:10.1016/j.dadm.2017.11.007
42. Friedman GD, Cutter GR, Donahue RP, et al. CARDIA: study design, recruitment, and some characteristics of the examined subjects. *J Clin Epidemiol*. 1988;41(11):1105–1116. [PubMed: 3204420]
43. Albert M, Soldan A, Gottesman R, et al. Cognitive changes preceding clinical symptom onset of mild cognitive impairment and relationship to ApoE genotype. *Curr Alzheimer Res*. 2014;11(8):773–784. [PubMed: 25212916]
44. Nasrallah IM, Pajewski NM, Auchus AP, et al. Association of Intensive vs Standard Blood Pressure Control With Cerebral White Matter Lesions. *JAMA*. 2019;322(6):524–534. doi:10.1001/jama.2019.10551 [PubMed: 31408137]



**Figure 1.** Flow chart showing the inclusion and exclusion criteria and final sample included in this study



## iSTAGING Dimensions in Cognitively Normal Subjects

**Figure 2.**

iSTAGING dimensions in cognitively normal subjects. A) SPARE-BA scores were calculated for n=8,284 subjects from 11 studies from the iSTAGING consortium using a supervised learning method. The model was applied with cross-validation using harmonized regional anatomical volumes of the subjects as input features. “Advanced” versus “resilient” aging groups were identified as individuals who deviated from normative aging trends. B) Subjects in “advanced” and “resilient” groups displayed widespread differences in atrophy patterns most pronounced in the frontal operculum, superior temporal, and insular cortex and further extending to frontal and inferior parietal cortex, as well as enlargement of the ventricles. C) SPARE-AD scores were calculated for n=5,460 subjects from 11 studies from the iSTAGING consortium using a supervised learning method. The model was trained using harmonized regional anatomical volumes as input features on ADNI CN and AD subjects and applied to all other studies; it was applied to ADNI subjects using cross-validation; D) Subjects with “high” and “low” SPARE-AD scores differed by atrophy patterns most pronounced in the hippocampus, amygdala, entorhinal cortex and inferior temporal cortex. E) White matter disease dimension, represented by white matter hyperintensities (WMH) as a function of age. WMH volume was calculated for n= 7,357

subjects from 10 studies using a deep learning method. F) Frequency maps of WMH in the iSTAGING consortium, showing WMH progression during the life span (in the 40s n=1,110, 50s n=1,918, 60s n=2,093, 70s n=1,330 and 80s n=321)

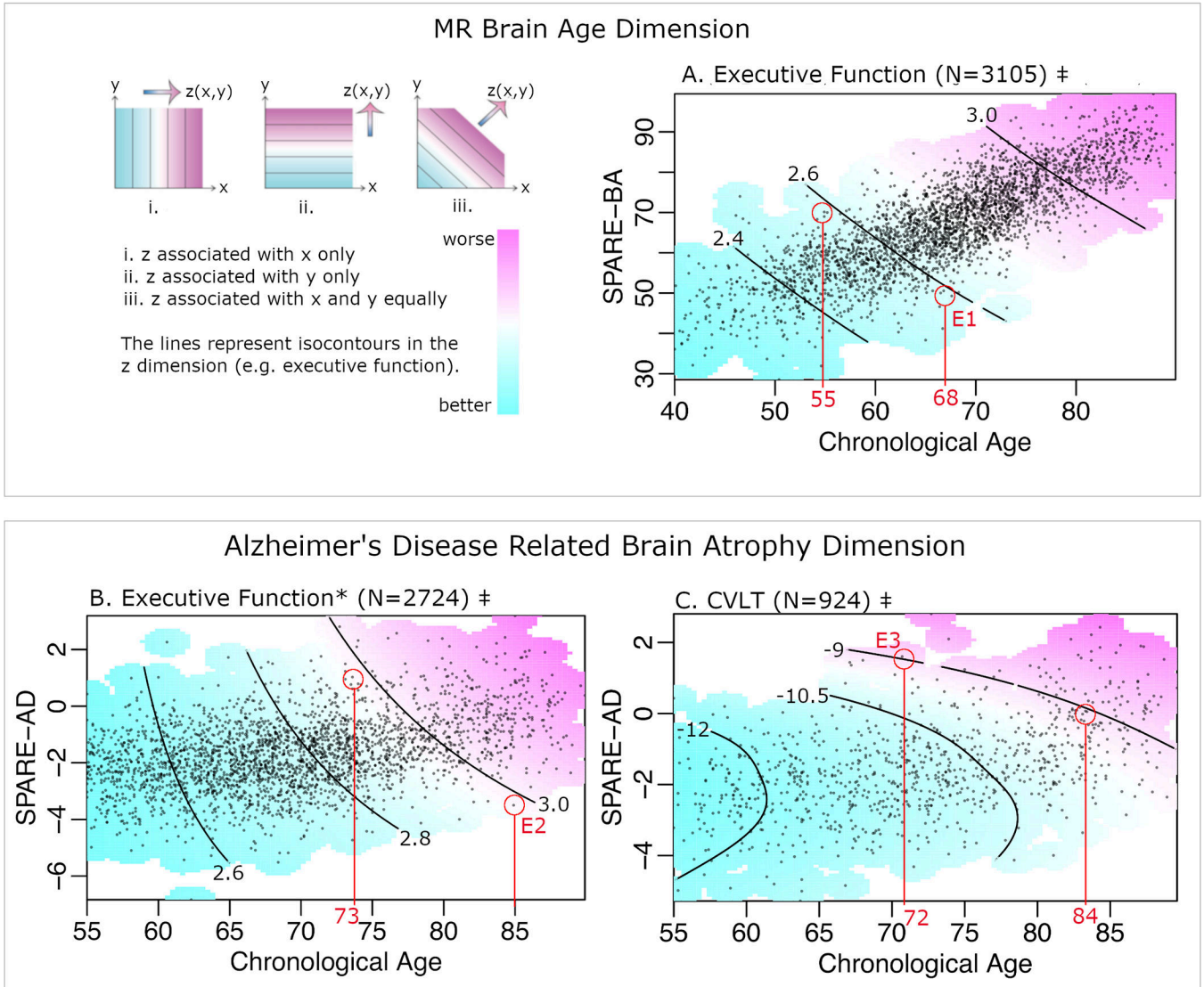
Author Manuscript

Author Manuscript

Author Manuscript

Author Manuscript

### Brain Charts of Aging and AD-like Atrophy in Cognitively Normal Subjects



†FDR corrected P-value <0.05, \*cubic root of (TMT-B - TMT-A)

**Interpretation Examples:**

- E1. 68 y.o. with 50 y.o.-like brain has the same executive function as 55 y.o. with 70 y.o.-like brain
- E2. 73 y.o. with high SPARE-AD has same executive function as 85 y.o. with low SPARE-AD
- E3. 72 y.o. with high SPARE-AD has same memory as 84 y.o. with low SPARE-AD

**Figure 3.**

A) Brain charts show associations between chronological age, SPARE-BA, and executive function. The relative diagonal isocontours indicate a similar contribution of age and SPARE-BA to the executive function (FDR corrected P-Value <0.05). Put differently, executive function at a given age cannot be estimated without SPARE-BA, and vice-versa.

B-C) Brain charts that show associations between chronological age, SPARE-AD, and cognitive testing. The isocontours of the executive function indicate a stronger association with age compared to SPARE-AD, but the effect of SPARE-AD was significant (FDR corrected P-Value <0.05) and increasing after the age of 65 years old. The isocontours of the

memory function showed a stronger association with SPARE-AD compared with age after the age of 70 years old, further underlying the role of AD-like atrophy on memory.

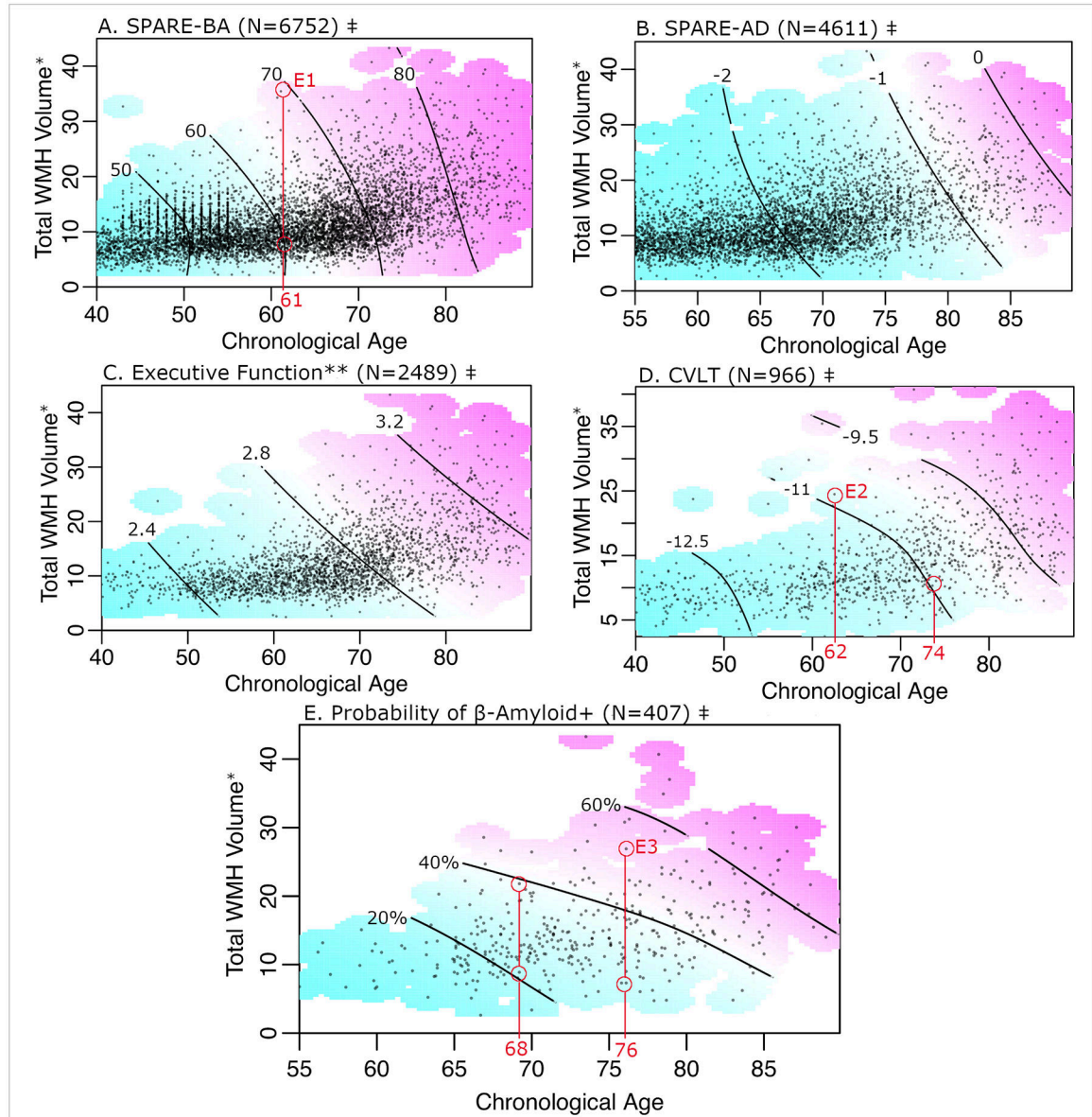
Author Manuscript

Author Manuscript

Author Manuscript

Author Manuscript

## White Matter Disease Dimension in Cognitively Normal Subjects



‡FDR corrected P-value <0.05, \*cubic root of White Matter Hyperintensity Volume measured in  $\text{mm}^3$ , \*\*cubic root of (TMT-B - TMT-A)

## Interpretation Examples:

E1. 39cc of WMH is associated with 10 years higher brain age (SPARE-BA), on average, to a 61 y.o.

E2. Low WMH is associated with maintained cognitive performance for 10+ years, on average

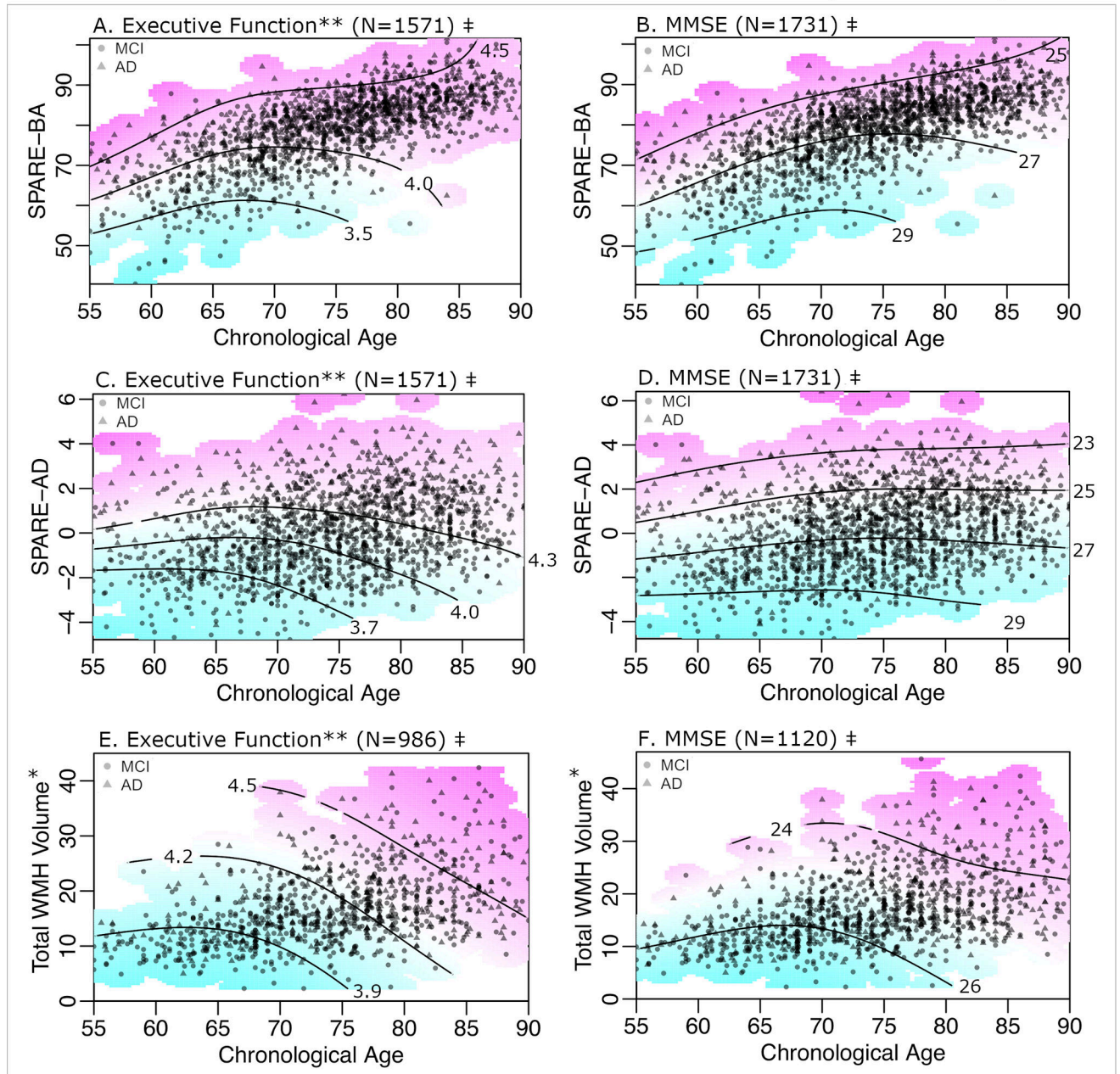
E3. WMH is associated with double the probability of testing positive for  $\beta$ -Amyloid

**Figure 4.**

A-B) Brain charts that show associations between chronological age, WMH volume, and brain atrophy captured with SPARE-BA and SPARE-AD. The isocontours of SPARE-BA and SPARE-AD indicate strong associations with WMH (FDR corrected P-Value <0.05 for both charts). C-D) Brain charts that show associations between chronological age, WMH volume, and cognitive testing. The isocontours of the executive function indicate strong associations with both age and WMH starting from the forties; the effect of WMH was significant (FDR corrected P-Value <0.05). The isocontours of the memory function showed

strong associations with age and WMH from the end of the forties; the effect of WMH was significant (FDR corrected P-Value <0.05). E) Brain charts that show associations between chronological age, WMH, and AD pathology. The isocontours of the A $\beta$  status showed strong associations with age and WMH from the sixties; the effect of WMH was significant (FDR corrected P-Value <0.05).

## Brain Charts in Patients with MCI and AD: Associations with Cognitive Testing Scores



‡FDR corrected P-value <0.05, \*cubic root of White Matter Hyperintensity Volume measured in  $\text{mm}^3$ , \*\*cubic root of (TMT-B - TMT-A)

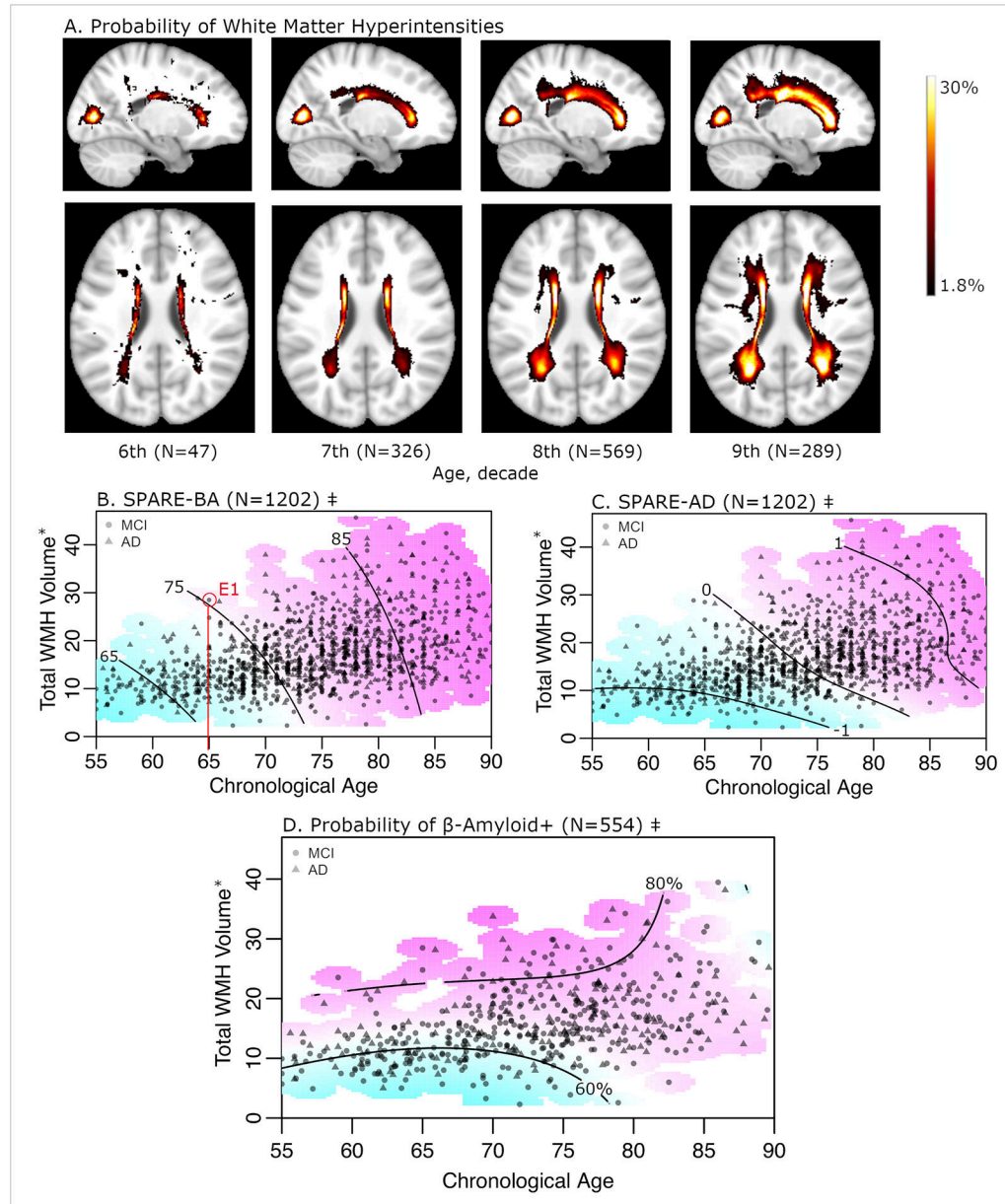
**Figure 5.**

Brain charts in patients with MCI and AD: Associations with cognitive testing scores. A-B) Brain charts that show associations between chronological age, predicted brain age (SPARE-BA), and cognitive testing. The isocontours of the executive function indicate a stronger association with SPARE-BA than with age (FDR corrected P-Value <0.05). Similarly, the isocontours of the memory function showed a stronger association with SPARE-BA compared with age; the effect of SPARE-BA was significant on memory (FDR corrected P-Value <0.05). C-D) Brain charts that show associations between chronological age, SPARE-

AD, and cognitive testing. The isocontours of the executive and memory functions indicate association with SPARE-AD only (horizontal isocontours); the effect of SPARE-AD was significant (FDR corrected P-Value <0.05). E-F) Brain charts that show associations between chronological age, WMH, and cognitive testing. The isocontours of the executive function indicate that the effect of WMH volume on executive function was relatively more pronounced at younger ages (relatively horizontal isocontours), whereas at older ages, both WMH and age are equal contributors to diminished executive function; the effect of WMH on executive function was significant (FDR corrected P-Value <0.05). The isocontours of the memory function showed stronger associations with WMH than age (FDR corrected P-Value <0.05)



Brain Charts in Patients with MCI and AD: the White Matter Disease Dimension



#FDR corrected P-value <0.05

\*cubic root of White Matter Hyperintensity Volume, measured in mm<sup>3</sup>

Interpretation Example:

E1. 30cc of WMH is associated with 10 years higher brain age (SPARE-BA), on average, to a 65 y.o.

**Figure 6.**

Brain charts in patients with MCI and AD: the WMH dimension. A) Frequency maps of WMH in the MCI and AD patients, showing WMH progression over age (in the 50s n=47, 60s n=326, 70s n=569, and 80s n=289). B-C) Brain charts that show associations between chronological age, WMH volume, and brain atrophy captured with SPARE-BA and SPARE-AD. The isocontours of SPARE-BA and SPARE-AD indicate strong associations with WMH (FDR corrected P-Value <0.05 for both charts). D) Brain chart that shows associations between chronological age, WMH, and AD pathology. The isocontours of the

A $\beta$  status showed stronger associations with WMH than age (FDR corrected P-Value <0.05).

Author Manuscript

Author Manuscript

Author Manuscript

Author Manuscript